Development of an IMU-Radar Sensor Board for Three-Dimensional Digital Image Correlation Camera Triangulation

Alessandro Sabato[a, *] and Christopher Niezrecki[a]
[a] Department of Mechanical Engineering, University of Massachusetts Lowell, 1 University Avenue, Lowell, MA, USA 01854

ABSTRACT

In the last few years, advancements made in cameras technology, optically-based systems, and computer-aided methods have made three-dimensional digital image correlation (3D-DIC) a robust tool for structural health monitoring (SHM) and extracting structural deformations and geometry profiles. To perform 3D-DIC measurements, the position of cameras relative to each other must be determined. It is achieved by taking several pictures of calibration objects to determine the camera's extrinsic parameters (i.e., separation distance and orientation in space). This practice can be very cumbersome and cameras calibration difficult to perform for large-sized structures. This is especially true if data is to be acquired from multiple fields of view. This study describes the design of a MEMS-based sensor board to extend 3D-DIC's capability and allow for easier calibration and measurement. The suggested system relies on a MEMS-based Inertial Measurement Unit (IMU) for determining the spatial orientation of the cameras (i.e., roll, pitch, and yaw angles) and a 77 GHz radar sensor for measuring the relative distance of the stereo cameras. Both systems are integrated on a commercially available microcontroller unit (MCU) that makes the system suitable for low-power applications. In this research, the efforts for programming the sensor board and the performance of the combined IMU-radar system in comparison with traditional instrumentation are described. To finish, the system is used for calculating the extrinsic parameters of a stereo-photogrammetry system and results are compared with data obtained from a traditional calibration.

Keywords: Digital Image Correlation, Inertial Measurement Unit, MEMS, Radar, Structural Health Monitoring

1. INTRODUCTION

The monitoring of civil, mechanical, and aerospace structures is essential, especially as many of these systems approach or surpass their design life. Therefore, the need to assess structural integrity is more important than ever and efficient and low-cost monitoring techniques are actively being sought. Often, Structural Health Monitoring (SHM) and Non-Destructive Inspection (NDI) of structures rely on sensing techniques for condition assessment. Advancements achieved in camera technology and optical sensors have made three-dimensional (3D) Digital Image Correlation (DIC) and three-dimensional point tracking (3DPT) valid techniques for extracting information about full-field displacement, strain, and geometry profiles of a variety of structures from images acquired using a pair of synchronized stereo-cameras. Among others examples, these techniques have been employed for monitoring the structural behavior of bridges[1], railroad tracks[2], wind turbine blades[3], and rotating machinery[4,5].

Photogrammetry and vision-based techniques use photographs recorded with imaging sensors to identify coordinates of points, features, and patterns of an object, and use this data to track their motion thorough different times or stages[6]. The fundamental principle of 3D-DIC is based on matching the same physical point between a reference state and the altered configuration. Before that, a calibration process needs to be performed by taking several images of an object containing optical targets whose positions are previously well-known. Thus, calibration is performed on the cameras' useful measurement volume to obtain the radial distortion coefficient together with the extrinsic and intrinsic parameters for each vision system[7]. The most straightforward technique used for calibration purposes only requires the camera(s) to observe a planar pattern shown in at least two different orientations[8]. Calibration for field of views up to ~2 meters are performed by taking several pictures of National Institute of Standards and Technology (NIST) - traceable calibration objects (e.g., panels or crosses) containing optical targets (i.e., dots) whose positions are previously well-known (see Figure 1a). A sequence of pictures of the calibration object at different distances and orientations is captured. Then a photogrammetry process known as bundle adjustment is used to establish the precise relationship between the two cameras. A ray-tracing method is implemented to find a unique intersection of points, similar to how a GPS triangulates coordinates. This procedure creates calibrated measuring volumes that are approximately the same width as the calibration object. This

* Alessandro_Sabato@uml.edu; phone +1 (978) 934-5253

information is required for computing the three elementary transformations needed for the pinhole camera model to obtain the 3D coordinate of any physical point using the triangulation theory[6, 9]. These include the conversion of global coordinates of a target object to the camera system coordinates, projection transformation into the retinal plane, and transformation into the sensor coordinate system in pixel units. Once a system is calibrated, the relative position of the cameras must not be altered. Otherwise, measurement errors will occur. Therefore, the camera pairs are rigidly mounted to a stiff bar (generally no longer than 3 m in length) or are fixed on stable tripods. A more complex calibration procedure needs to be performed if the dimensions of the targeted object increase (i.e., large-area calibration)[10, 11]. This operation is arduous as it involves the use of coded and un-coded targets that have to be placed on an area having dimensions comparable to that of the object to be tested (see Figure 1b).

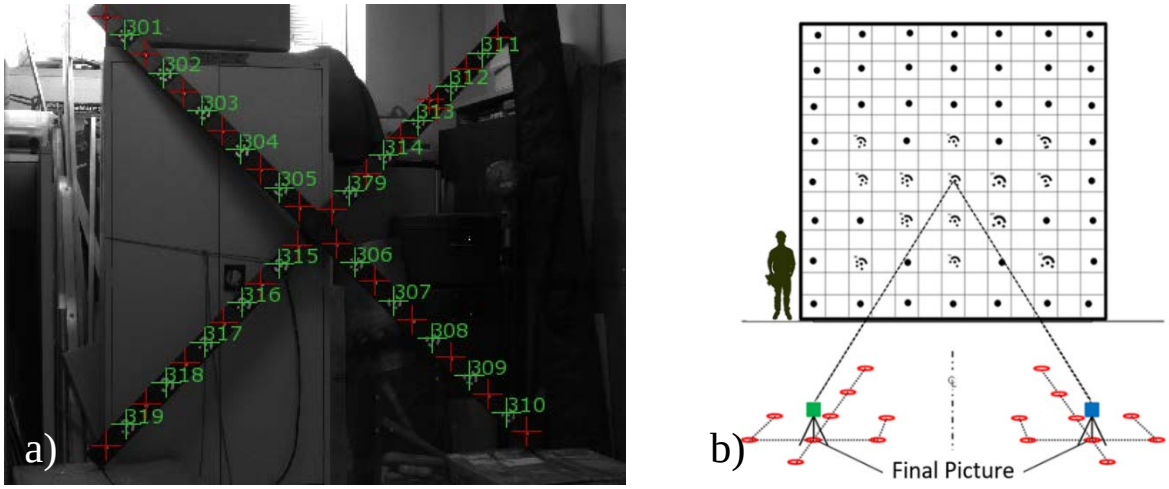

Figure 1. a) Example of calibration target recognition on a coded calibration cross having dimension of 2m x 2m; b) Schematic of a large-area calibration procedure using 14 coded and 42 un-coded targets over a calibration surface with dimensions of approximately 7m x 7m

An example of large area calibration is provided in Figure 1b, where the schematic of a customized calibration panel used for a surface with dimensions of 7m x 7m is shown. During the process, the calibration of the first camera has to be performed by taking images from 12 different views of the target array (i.e., the red circles in Figure 1b); then, the same procedure is repeated for twelve more pictures to be taken with the second camera. Finally, the last images of the calibration panel array are recorded using both cameras in their final relative position. As can be imagined, this procedure is time-consuming also because the distance between several pairs of targets needs to be measured to be used as scale bars. Moreover, once the last picture is taken, the location of one camera with respect to the other cannot change; otherwise, it will affect the calculated extrinsic parameters values, and it would result in a loss of calibration. The fabrication of the required calibration panel or camera bar, the sensitivity of the cameras to relative motion, and the manpower involved in the process and its complexity, make the current large-area calibration procedure difficult and not practical to perform SHM, NDI, and dynamic testing of larger-scale structures such as bridges, wind turbines, and tall buildings.

To address this yet unresolved issue, a group of researchers at the University of Massachusetts Lowell has developed a prototype of a wireless multi-sensor system that can change the way SHM is done for large structures. By using off-the-shelf components integrated on a microcontroller unit (MCU), a sensor board has been developed to be installed on each of the cameras to determine the seven degrees-of-freedom (DOFs) needed to identify the cameras' relative position. The 7 DOFs include: (1) the distance between the cameras, (2, 3, 4) roll, pitch, and yaw of camera #1, and (5, 6, 7) roll, pitch, and yaw of camera #2. The developed multi-sensor system and associated MCU embeds a MEMS-based Inertial Measurement Unit (IMU) for roll, pitch and yaw detection and a 77 GHz radar unit for determining the distance between the cameras in space[12].

In this paper, the laboratory tests performed to evaluate the measurement accuracy of the IMU sensor board in comparison with traditional instrumentation are described. Lastly, the system is used for calculating the extrinsic parameters of a stereo-photogrammetry system and results are compared with data obtained from a traditional 3D-DIC calibration. If fully

developed, the proposed system would enable to achieve easier measurements on large-scale engineering structures and infrastructure that require periodic inspections.

2. EVALUATION OF THE ACCURACY OF THE IMU SENSOR

An IMU is an electronic device that can measure a body's acceleration, angular rotation, and magnetic heading, using a combination of accelerometers, gyroscopes, and magnetometers. The accelerometer is used to detect the components of the acceleration of gravity and those data can be used for calculating pitch and roll. The gyroscope's data provide a rate of rotation or relative motion, but not an absolute position (x, y, z). Therefore, the motion vectors can be integrated to estimate change from a known position, while the magnetometer can be used for detecting the change in the magnetic field to determine rotation from the North. In this paper, due to an unclear interference causing excessive noise in the data recorded using the magnetometer, the value of the roll, pitch, and yaw angles are determined using the reading of the three-axis accelerometer embedded in the IMU by employing a game rotation approach rather than relying on the geomagnetic rotation vector[13, 14].

To characterize the proposed system, some preliminary tests have been performed. In this research, the IMU sensitivity (i.e., an ICM-20948 sensor produced by InvenSense[15]) has been assessed by performing a back-to-back comparison with another device (i.e., a commercially available app for activating the tiltmeter embedded in an iPhone 5S cellphone). This paragraph, focuses on those tests performed for assessing the accuracy of the IMU sensor board in measuring the roll, pitch and yaw angles, while for a description of the tests performed on the Radar system, together with a description of how the IMU is integrated on the sensor board, the interested reader can refer to the paper[12].

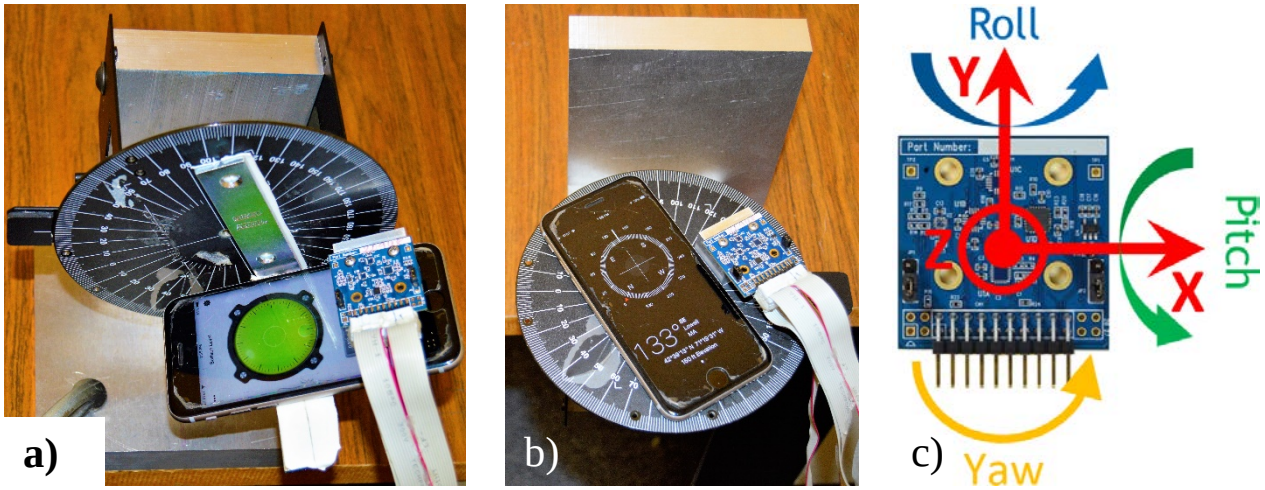

Figure 2. Experimental setup for IMU characterization and back-to-back comparison with the inclinometer embedded in a cellphone: a) roll angle characterization setup; b) yaw angle characterization setup; c) schematic of sensing axes of the IMU.

The accuracy of the IMU has been determined by rotating the sensor and subjecting to measure the different components of the acceleration of gravity through three perpendicular axes. Recorded values have been used in a back-to-back comparison with an inclinometer application embedded in a cellphone. During the tests, the IMU and cellphone have been attached to a rotation stage in a setup similar to that shown in Figure 2 for changing their orientation in space.

2.1 Pitch angle accuracy

For assessing the accuracy of the IMU in detecting the changes in the pitch angle, the rotation stage has been rotated with 5° increments from 60° to -60°. For each position, data for 30 seconds has been recorded to allow data averaging and significant statistical parameters evaluation. Static acceleration data recorded have been used for calculating the values of pitch using equation (1) and are compared with the reading from the cellphone as summarized in Figure 3.

$$\theta_{pitch} = \tan^{-1} \frac{Acc_X}{\left(\sqrt{Acc_Y^2 + Acc_Z^2}\right)} \quad (1)$$

where Acc_X, Acc_Y, and Acc_Z are the static acceleration recorded in the *X*, *Y*, and *Z* directions respectively.

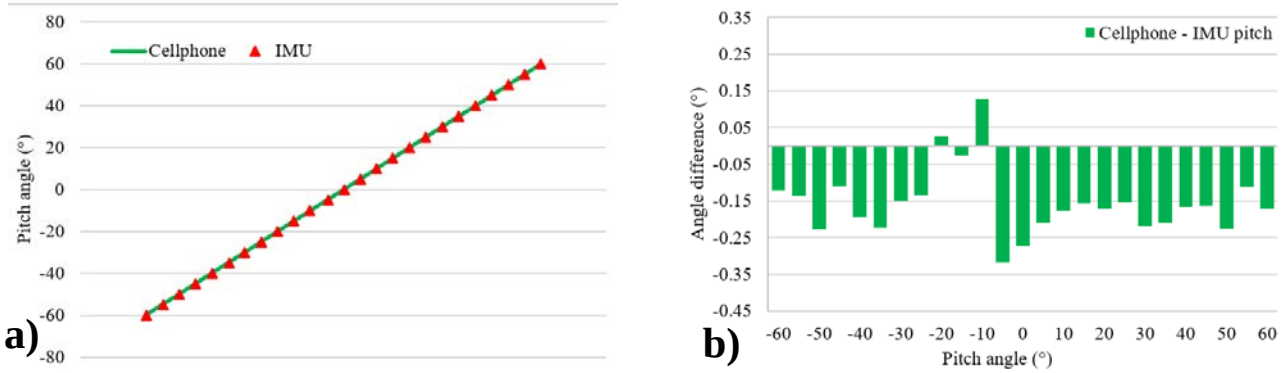

Figure 3. Comparison of pitch angles measured using the cellphone (continuous green line) and the IMU sensor (dotted red line): a) Angle measured for different orientations of the translation stage and b) difference between the values measure using the two devices as the pitch angles vary.

Results plotted in Figures 3a and 3b show an excellent agreement between the IMU and cellphone data for different values of the pitch angle. From a more accurate analysis, it is observed that the difference between the two data sets is usually in the range ± 0.350°, with an absolute average error equal to 0.168°. This value confirms the good accuracy of the IMU sensor, especially when the accuracy of the reference cellphone in measuring pitch and tilt angles is considered (i.e., ± 0.1°).

2.2 Roll angle accuracy

Similar to what done for the pitch angle, the IMU and the cellphone have been rotated along the sensors' Y-axis for subjecting the systems to different values of the static acceleration of gravity and thus, simulating different values for the roll angle. During this test, the rotation stage has been rotated with 5° increments from 60° to -60°. For each position, 30 seconds of readings have been recorded to allow data averaging and significant statistical parameters evaluation. Static acceleration data recorded have been used for calculating the values of the roll angle using equation (2) and are compared with the reading from the cellphone as summarized in Figure 4.

$$\theta_{roll} = \tan^{-1} \frac{Acc_Y}{\left(\sqrt{Acc_X^2 + Acc_Z^2}\right)} \quad (2)$$

where the terms introduced have the same definition as described for Eq. (1).

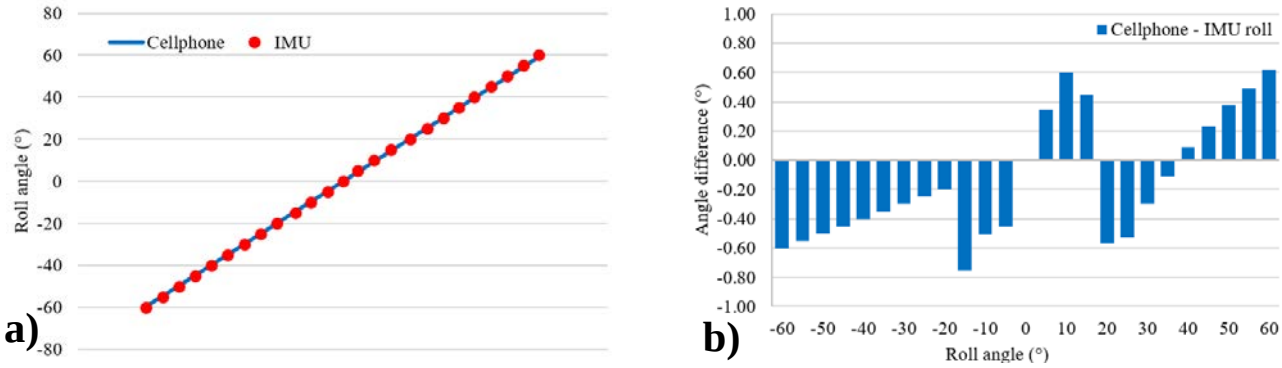

Figure 4. Comparison of roll angles measured using the cellphone (continuous blue line) and the IMU sensor (dotted red line): a) Angle measured for different orientations of the translation stage and b) difference between the values measure using the two devices as the roll angles vary.

From the analysis of the results shown in Figure 4, it is observed that the values vary on a larger interval when compared with the previous example (i.e., ± 0.600° compared to ± 0.350°, with some highs close to –0.800°). Besides, it is observed that the difference between the data recorded using the IMU and those recorded using the cellphone increases as the angle increases as well. This can be due to some instabilities in the rotation stage used for simulating the angle variation and in some data drifting phenomena in the cellphone (i.e., the angle measured with the cellphone did not remain constant during each test). Nonetheless, still, a good correlation is observed between the two data sets with an absolute average error equal to 0.400°.

2.3 Yaw angle accuracy

To finish, the cellphone and the IMU have been subjected to variation in the yaw angle by using the setup shown in Figure 2b. In this test, the IMU and the cellphone have been rotated along the sensors' Z-axis with 10° increments from 0° to 180°. For each position, a 30 second reading has been recorded to allow data averaging and significant statistical parameters evaluation. The data measured using the compass embedded in the cellphone and those sampled using the IMU and processed using equation (3) and are shown in Figure 5.

$$\theta_{yaw} = \tan^{-1} \frac{Acc_Z}{\left(\sqrt{Acc_X^2 + Acc_Z^2}\right)} \tag{3}$$

where the terms have the same definition as described for Eq. (1).

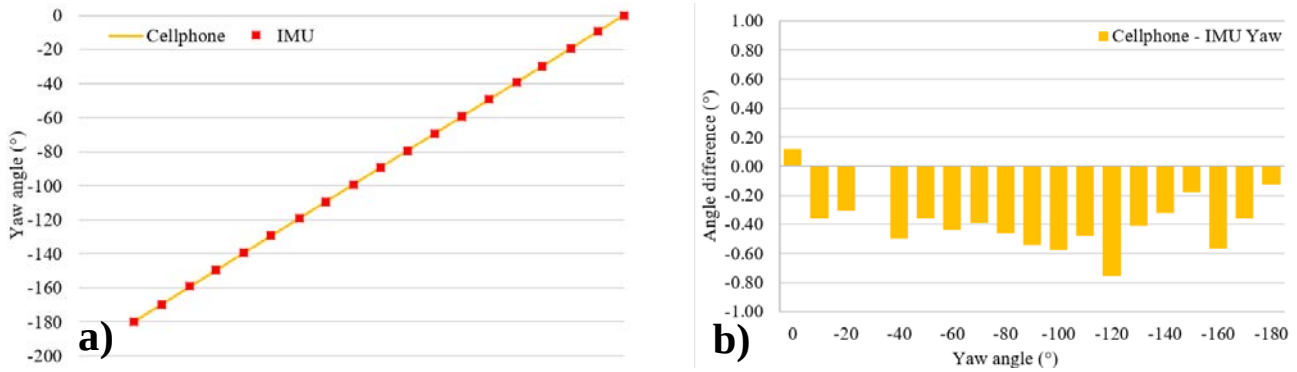

Figure 5. Comparison of yaw angles measured using the cellphone (continuous yellow line) and the IMU sensor (dotted red line): a) Angle measured for different orientations of the translation stage and b) difference between the values measure using the two devices as the yaw angles vary.

The results plotted in Figure 5 show an excellent agreement between the IMU and cellphone data for different values of the yaw angle. From a more accurate analysis, it is observed that the difference between the two data sets is usually in the range ± 0.500°, with a peak value of -0.760° at 120°, and an absolute average error equal to 0.382°. This value confirms the good accuracy of the IMU, especially when the sensitivity of the compass in the cellphone (i.e., ± 1°) used for determining the interval of rotation of the translation stage is considered.

3. ACCURACY OF THE IMU-RADAR SENSOR IN DETERMINIG EXTRINSIC PARAMETERS

The second part of this study focuses on evaluating the accuracy of the sensor board described in [15] to calculate the position of two remotely paired cameras that are used for performing a 3D-DIC measurement. For doing this, a set of laboratory tests have been performed to measure the cameras relative position by performing a traditional calibration procedure as described in[7]. This approach relies on a number of pictures of a reference object taken from different views to calculate the intrinsic (e.g., focal length) and extrinsic (i.e., base distance and separation angle) parameters of the stereophotogrammetry system[8, 16]. This research focuses mainly on the determination of the extrinsic parameters, as the

intrinsic ones are stored as meta-information each time a picture is taken using a digital camera. In this study, a coded calibration cross having dimensions of 2 m x 2 m was used in conjunction with a pair of cameras installed on a rigid metal bar. In particular, two 2 Megapixel FWX201 series digital cameras manufactured by Baumer GmBH employing a 1/1.8″ interline progressive charge coupled device (CCD) monochrome image sensors with a resolution of 1626 × 1236 pixels and a pixel size of $4.4 \times 4.4 \cdot 10^{-6}$ m, fitted with 12 mm focal length lenses were used in the study[17]. The 3D DIC system was positioned to have a working distance of nearly 4.5 m from the coded cross, and a base distance and separation angle to be determined experimentally. An overview of the calibration setup is shown in Figure 6.

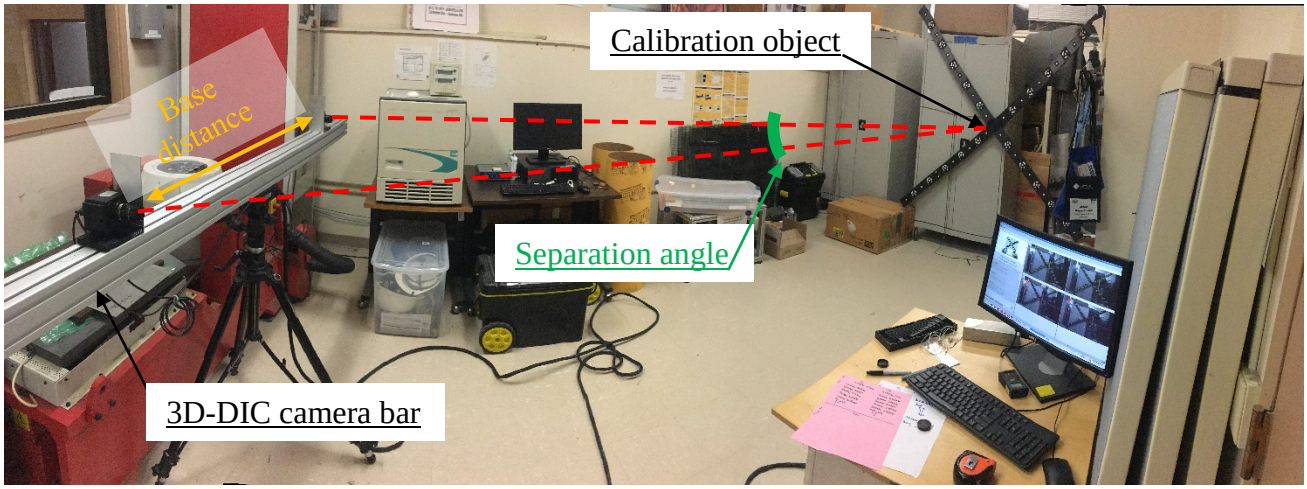

Figure 6. Experimental setup used for determining the stereophotogrammetry system extrinsic parameters using a traditional procedure.

By taking 28 pictures of the calibration object shown in Figure 6, and processing the images using the commercially available software Aramis by GOM, a separation angle equal to 24.6° has been calculated for the selected configuration. Then, the developed IMU-Radar sensor board has been installed on the rigid metal bar and used for measuring the angle that the two cameras' line of sight formed with the direction perpendicular to metal support attached to the bar and their mutual distance. The setup used for performing this test is shown in Figure 7.

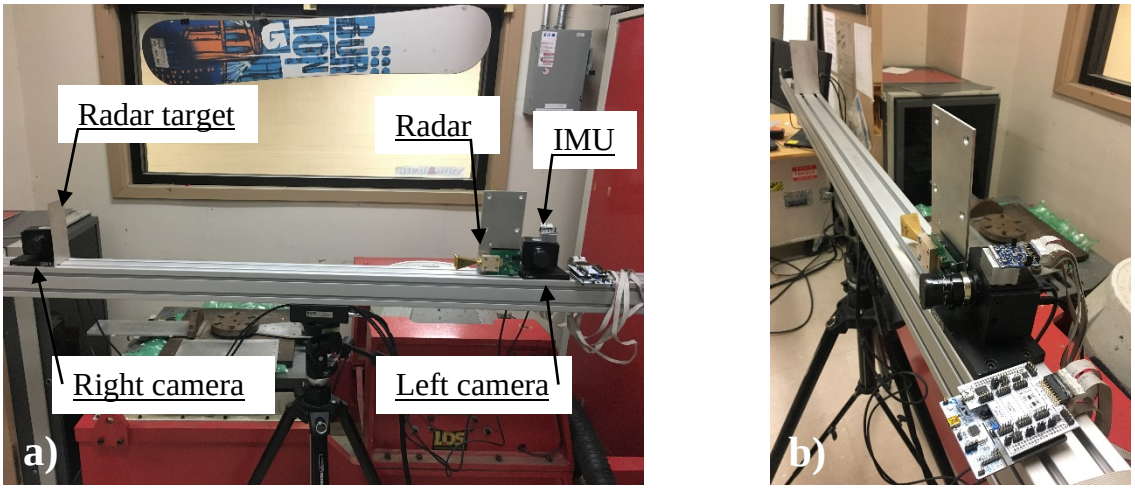

Figure 7. Experimental setup used for measuring the extrinsic parameters of the stereophotogrammetry system using the IMU-Radar sensor board: a) Front view with the radar unit and the IMU sensor in correspondence of the left camera; b) detail of the sensor deployment with metal target located on the right camera for measuring the relative distance with the radar.

By using the IMU-Radar sensor board, the angle that the left and right cameras measure with respects to the perpendicular direction of the metal connection with the bar is equal to 12.8° and 12° respectively. Therefore, the separation angle between the two cameras is 24.8°. This value is very similar from the 24.6° computed using the Aramis software via the traditional calibration procedure. The small difference can be due to noise in the signal sampled using the IMU (that is processed without performing any filtering or other signal processing manipulations) or by a non-perfect alignment between the sensor and the edges of the cameras. Also, a base distance of 1.9765 m is measured using the radar. By combining these two values, it is possible to determine the distance of the common focal point of the two cameras located 4.495 m away from the metal bar.

4. CONCLUSIONS

A novel sensor board prototype is proposed for measuring the seven degrees of freedom (i.e., the distance between the cameras, roll, pitch and yaw of camera #1, and roll, pitch, and yaw of camera #2) necessary for determining the extrinsic parameters of a set of paired cameras to be used for performing three-dimensional digital image correlation (3D-DIC). The system consists of an inertial measurement unit (IMU) and a 77 GHz radar unit embedded on a Raspberry Pi 3 microcontroller unit (MCU) board. In this study, the characterization of the IMU sensor is introduced, and a comparison with the IMU sensor embedded in a cellphone is performed. Moreover, a direct comparison between the extrinsic parameters measured using the proposed device and those computed using a traditional procedure based on the analysis of several views of a coded calibration object is presented.

Many laboratory experiments have shown that the accuracy of the IMU can detect values of pitch, roll, and yaw angles with an average accuracy of 0.168°, 0.400°, and 0.382° respectively when a back-to-back comparison with an inclinometer embedded in a smartphone is performed. Moreover, when the data retrieved using the proposed sensor board are compared with those calculated using traditional photogrammetry approaches, good correlation is shown. In the example shown in this research, a difference equal to 0.2° is found between the separation angle calculated using the two systems.

Nonetheless, results are extremely encouraging and may pave the road to further development. The proposed system has the potential to transform the way existing small-scale photogrammetry and DIC measurements are made and will also enable quantitative analyses to be made at very-large-scale (>100 m) from multiple angles and positions. The final product will be able to measure the position of two cameras in space in real-time for providing their relative distance and orientation and store this information for each picture taken. Then collected data will be used for performing the 3D-DIC or 3DPT measurement by triangulating the position of a target object with respect to the two cameras and determining its displacement at every stage. The proposed calibration system will also be insensitive to camera movement and therefore can be attached to a pair of unmanned aerial vehicles (UAVs) to enable measurement from multiple locations and fields of view. The use of the proposed system may allow the self-calibration of cameras as 3D-DIC analyses have to be performed eliminating the need for a rigid bar connection between the cameras, streamlining the calibration process, and extending the range of applicability that stereophotogrammetry and DIC can have. The use of the self-calibration sensor board will eliminate the need for a rigid bar connection between the cameras, extending the range of applicability of stereophotogrammetry and DIC. Successful completion of the proposed system has the potential to make the currently used photogrammetry calibration process obsolete, as it will allow each image pair to have its own calibration file. The proposed method could become a structural evaluation tool that will enable cost-effective and reduce time-consuming inspections while providing quantitative measurements beyond what a single camera can offer.

REFERENCES

[1] Reagan, D., Sabato, A., and Niezrecki, C., “Unmanned aerial vehicle acquisition of three-dimensional digital image correlation measurements for structural health monitoring of bridges,” Proc. SPIE Smart Structures and Materials+ Nondestructive Evaluation and Health Monitoring, Portland, OR, (2017).

[2] Sabato, A., and Niezrecki, C., “Feasibility of digital image correlation for railroad tie inspection and ballast support assessment,” Measurement, 103, 93-105 (2017).

[3] LeBlanc, B., Niezrecki, C., Avitabile, P., Chen, J., and Sherwood, J., “Damage detection and full surface characterization of a wind turbine blade using three-dimensional digital image correlation,” Structural Health Monitoring, 12(5-6), 430-439 (2013).

[4] LeBlanc, B., Niezrecki, C., Avitable, P., and Tribikram, K., "Structural health monitoring of helicopter hard landing using 3D digital image correlation," Proc. SPIE Smart Structures and Materials+ Nondestructive Evaluation and Health Monitoring, (2010).
[5] Niezrecki, C., Baqersad, J., and Sabato, A., "Digital image correlation techniques for NDE and SHM," Handbook of Advanced Non-Destructive Evaluation, 1-46 (2018).
[6] Sutton, M. A., Wolters, W. J., Peters, W. H., Ranson, W. F., and McNeill, S. R., "Determination of displacements using an improved digital correlation method," Image and vision computing, 1(3), 133-139 (1983).
[7] Schmidt, T., Tyson, J., and Galanulis, K., "Full-field dynamic displacement and strain measurement using advanced 3d image correlation photogrammetry: part 1," Experimental Techniques, 27(3), 47-50 (2003).
[8] Zhang, Z., "A flexible new technique for camera calibration," IEEE Transactions on pattern analysis and machine intelligence, 22(11), 1330-1334 (2000).
[9] Sturm, P., "Pinhole camera model," Computer Vision (pp. 610-613). Springer US, (2014).
[10] Poozesh P., Baqersad J., Niezrecki C., Avitabile P., Harvey E., and Yarala R., "Large-area photogrammetry based testing of wind turbine blades," Mech Syst Signal Process, 86: 98-115 (2017).
[11] Sabato A., Poozesh P., Avitabile P., Niezrecki C., "Experimental modal analysis of a utility-scale wind turbine blade using a multi-camera approach,", Proc.13th AIVELA, June 19-22, Ancona, Italy (2018)
[12] Sabato, A., Reddy, N., Khan, S., and Niezrecki, C., "A novel camera localization system for extending three-dimensional digital image correlation," Proc. SPIE Smart Structures and Materials+ Nondestructive Evaluation and Health Monitoring, Denver, CO (2018).
[13] Haslwanter, T., "Mathematics of three-dimensional eye rotations," Vision research, 35(12), 1727-1740 (1995).
[14] Weisstein, E. W., "Rotation matrix", http://mathworld.wolfram.com/RotationMatrix.html, (2003)
[15] ICM-20948 - World's lowest power 9-axis MotionTracking device, Available online: https://www.invensense.com/products/motion-tracking/9-axis/icm-20948/ (Accessed February 2019).
[16] Heyden, A., and Astrom, K., "Euclidean reconstruction from constant intrinsic parameters," Proc. 13th International Conference on Pattern Recognition, 1996.
[17] Baumer. FWX20C NeuroCheck Edition – Digital Color Progressive Scan Camera. <http://rhengineering.de/wp-content/uploads/2015/07/Baumer_FWX20c_NC_v10e_041013.pdf> (Accessed February 2019).